An Exponential Decay Model for the Deterministic Correlations in Axial Compressors

Yangwei Liu[1,2]*, Baojie Liu[1,2], Lipeng Lu[1,2]

ISROMAC 2017

International Symposium on Transport Phenomena and Dynamics of Rotating Machinery

Hawaii, Maui

December 16-21 2017

Abstract

The average-passage equation system (APES) provides a rigorous mathematical framework to account for the UBRI in steady state environment by introducing the deterministic correlations (DC). How to model the DC is the key in APES method. The primary purpose of this study is to develop a DC model for compressor routine design. A 3D viscous unsteady and time-averaging CFD flow solver is developed to investigate the APES technique. Steady, unsteady and time-averaging simulations are conducted on the investigation of the UBRI in the first stage of NASA 67 compressor. Based on DC characteristics and its effects on time-averaged flow, an exponential decay DC model is proposed and implemented into the time-averaging solver. Based on the unsteady simulation, the proposed model is validated by comparing DC distributions and mean flow fields. The comparison indicates that the proposed model can take into account the major part of UBRI and provide significant improvements for predicting spanwise distributions of flow properties in axial compressors, compared with the steady mixing plane method.

Keywords

Exponential Decay Model —Deterministic Correlations —APES —CFD —Axial Compressors

[1] *National Key Laboratory of Science and Technology on Aero-Engine Aero-Thermodynamics, School of Energy and Power Engineering, Beihang University, Beijing 100191, China;*

[2] *Collaborative Innovation Center of Advanced Aero-Engine, Beihang University, Beijing 100191, China*

*__Corresponding author__: liuyangwei@126.com

INTRODUCTION

The flow within turbomachinery is inherently unsteady and the unsteady blade row interaction (UBRI) has a large impact on turbomachinery performance. However, unsteady calculations are still too time consuming for use in routine design and so steady mixing plane method that neglects UBRI is widely used [1]. A steady simulation taking the unsteadiness into account may be a solution of this tricky problem. By applying three averaging operators (ensemble, time and passage averaging operator) to Navier-Stokes equations, Adamczyk proposed the average-passage equation system (APES) [2], which could provide a rigorous mathematical framework for accounting for the UBRI in steady state calculation by introducing deterministic correlations (DC). The DC in momentum equation are called deterministic stresses (DS) and the DC in energy equation are called deterministic enthalpy fluxes (DEF). How to model the DC to close the equation system is the key in the APES.

In recent years, many efforts have been made and some DC models have been proposed [3-11]. Some DC models [3-5,8] are axisymmetric based on a hypothesis that the purely unsteady fluctuations are negligible, though the DC is not uniform in circumferential direction and the gradients are large in some regions in the blade passage [12]. Adamczyk et al. [3] proposed the first model using overlapping grids for all blade rows without the interface planes. Rhie et al. [4] developed a continuous interface plane approach using overlapping grids for downstream row only. Based on an enhanced wake decay concept, Hall [8] proposed a deterministic mixing-stress model within the framework of “mixing-plane”-type prediction scheme and could be easily implemented.

Some DC models could present circumferential distributions [6,7,9-11]. Some reduced order models by simplified unsteady calculations were proposed [6,7], and are still time consuming in comparison with the mixing plane method. Sondak et al. [6] developed a “lumped” DC model based on lower-order (inviscid) time-dependent simulations and the model saved 63 percent the CPU time compared with unsteady viscous simulation. He [7] developed a nonlinear harmonic method that is much more efficient than the unsteady time-marching methods while still modeling the dominant nonlinear effects. Van de wall [9] proposed a transport model that can take into account the effects related to slicing of the upstream wakes by a downstream blade row. Charbonnier & Leboeuf [10] found that the velocity-pressure gradient correlation is a key parameter for the transport model and proposed a closure for this correlation term. Only DS in momentum equations are modeled in the transport models [8-11], though there are also DEF in energy equation.

The above studies showed that the models employed in the APES obviously improved the numerical results in comparison with the mixing plane method. However, none of these DC models has been widely used in the multistage compressor routine design because these models are either too complex, too temperamental or still too time consuming for routine use. Hence, more research work for modeling the DC should be conducted. In our previous studies, the distribution characteristics of DC and the effects of DC on time-averaging simulation were conducted [12-16]. We found that the time-averaging simulation with axisymmetric DC can take into account the major part of the unsteady effects on spanwise

redistribution. The time-averaging simulation with either DS or DEF can only reproduce a partial influence of unsteady blade row interactions on time-averaged flow. Hence, both DS and DEF should be modeled in the APES approach.

In this paper, the purpose is to propose a DC model that fits compressor routine design. Firstly, a 3D viscous unsteady and time-averaging CFD flow solver is developed to investigate the APES technique. Secondly, steady, unsteady and time-averaging simulations are conducted on the investigation of the UBRI, DC distribution characteristics, and the influence of DC on the time-averaged flow field in axial compressors. Lastly, an exponential decay DC model is proposed and validated.

1. METHODS

A 3D viscous unsteady and time-averaging CFD flow solver is developed to investigate the APES technique. Then steady, unsteady and time-averaging simulations are conducted on the investigation of the UBRI in the first transonic stage of NASA 67 at design condition. Based on the studies of DC distribution characteristics, and the influence of DC on the time-averaged flow field, an exponential decay DC model is proposed and validated.

1.1 Numerical Solver

The unsteady and time-averaging CFD flow solver was developed based on the Denton steady code [17]. The time-averaging CFD flow solver, adopting APES, was developed to account for the unsteady blade row interactions within the framework of a continuous interface plane approach. The numerical methods were improved to enhance the accuracy, convergence and flexibility, including grid generations, spatial/temporal discretisation of governing equations, boundary conditions and acceleration techniques [18].

The form of the APES used in this study was developed through the consecutive application of ensemble averaging operator and time averaging operator (see Adamczyk [2]) applied to the Navier-Stokes equation, the same form as that used by Hall [8]. The integral form of the time-averaging equations in cylindrical coordinates are:

$$\begin{aligned}&\frac{\partial}{\partial\tau}\iiint_{\Omega} U d\Omega \\ &+\oint_{\partial\Omega}\left((F_c-F_v+F_d)\vec{i}+(G_c-G_v+G_d)\vec{j}+(H_c-H_v+H_d)\vec{k}\right)\cdot d\vec{S} \\ &=\iiint_{\Omega}(Q+Q_d)d\Omega\end{aligned} \tag{1}$$

where U, F_c, G_c, H_c and Q are conservative variable and inviscid flux vectors. F_v, G_v and H_v are viscid flux vectors. F_d, G_d, H_d and Q_d are deterministic flux vectors, which are extra terms compared to the steady flow equations.

$$[U,F_c,G_c,H_c]=\begin{bmatrix}\bar{\rho} & \bar{\rho}V_x & \bar{\rho}V_r & \bar{\rho}W_\theta \\ \bar{\rho}V_x & \bar{\rho}V_xV_x+\bar{p} & \bar{\rho}V_rV_x & \bar{\rho}W_\theta V_x \\ \bar{\rho}V_r & \bar{\rho}V_xV_r & \bar{\rho}V_rV_r+\bar{p} & \bar{\rho}W_\theta V_r \\ r\bar{\rho}V_\theta & r\bar{\rho}V_xV_\theta & r\bar{\rho}V_rV_\theta & r(\bar{\rho}W_\theta V_\theta+\bar{p}) \\ \bar{\rho}E & \bar{\rho}V_x\overline{H} & \bar{\rho}V_r\overline{H} & \bar{\rho}W_\theta\overline{V_r}+r\omega\bar{p}\end{bmatrix} \tag{2}$$

$$[F_v,G_v,H_v]=\begin{bmatrix}0 & 0 & 0 \\ \overline{\tau_{xx}} & \overline{\tau_{xr}} & \overline{\tau_{x\theta}} \\ \overline{\tau_{rx}} & \overline{\tau_{rr}} & \overline{\tau_{r\theta}} \\ r\overline{\tau_{\theta x}} & r\overline{\tau_{\theta r}} & r\overline{\tau_{\theta\theta}} \\ e_1 & e_2 & e_3\end{bmatrix} \tag{3}$$

$$\begin{bmatrix}e_1\\e_2\\e_3\end{bmatrix}=\begin{bmatrix}\overline{\tau_{xx}} & \overline{\tau_{xr}} & \overline{\tau_{x\theta}} \\ \overline{\tau_{rx}} & \overline{\tau_{rr}} & \overline{\tau_{r\theta}} \\ \overline{\tau_{\theta x}} & \overline{\tau_{\theta r}} & \overline{\tau_{\theta\theta}}\end{bmatrix}\begin{bmatrix}V_x\\V_r\\V_\theta\end{bmatrix}+\lambda\begin{bmatrix}\dfrac{\partial T}{\partial x}\\ \dfrac{\partial T}{\partial r}\\ \dfrac{\partial T}{r\partial\theta}\end{bmatrix} \tag{4}$$

$$Q=\frac{1}{r}\begin{bmatrix}0\\0\\\bar{p}+\bar{\rho}V_\theta{}^2\\0\\0\end{bmatrix}+\frac{1}{r}\begin{bmatrix}0\\0\\-\overline{\tau_{\theta\theta}}\\0\\0\end{bmatrix} \tag{5}$$

$$[F_d,G_d,H_d]=\begin{bmatrix}0 & 0 & 0 \\ \bar{\rho}V_x''V_x'' & \bar{\rho}V_r''V_x'' & \bar{\rho}V_\theta''V_x'' \\ \bar{\rho}V_x''V_r'' & \bar{\rho}V_r''V_r'' & \bar{\rho}V_\theta''V_r'' \\ r\bar{\rho}V_x''V_\theta'' & r\bar{\rho}V_r''V_\theta'' & r\bar{\rho}V_\theta''V_\theta'' \\ \overline{\bar{\rho}V_x''H''+\bar{e}_1} & \overline{\bar{\rho}V_r''H''+\bar{e}_2} & \overline{\bar{\rho}V_\theta''H''+\bar{e}_3}\end{bmatrix} \tag{6}$$

$$\begin{bmatrix}\bar{e}_1\\\bar{e}_2\\\bar{e}_3\end{bmatrix}=\begin{bmatrix}\overline{\tau_{xx}''V_x''}+\overline{\tau_{xr}''V_r''}+\overline{\tau_{x\theta}''V_\theta''} \\ \overline{\tau_{rx}''V_x''}+\overline{\tau_{rr}''V_r''}+\overline{\tau_{r\theta}''V_\theta''} \\ \overline{\tau_{\theta x}''V_x''}+\overline{\tau_{\theta r}''V_r''}+\overline{\tau_{\theta\theta}''V_\theta''}\end{bmatrix} \tag{7}$$

$$Q_d=\frac{1}{r}\begin{bmatrix}0\\0\\\bar{\rho}V_\theta''V_\theta''\\0\\0\end{bmatrix} \tag{8}$$

$$E=c_vT+\frac{1}{2}\bar{\rho}(V_x{}^2+V_r{}^2+V_\theta{}^2)+\frac{1}{2}\bar{\rho}(V_x''V_x''+V_r''V_r''+V_\theta''V_\theta'') \tag{9}$$

$$\begin{aligned}H&=E+\frac{\bar{p}}{\bar{\rho}}\\ &=c_pT+\frac{1}{2}\bar{\rho}(V_x{}^2+V_r{}^2+V_\theta{}^2)+\frac{1}{2}\bar{\rho}(V_x''V_x''+V_r''V_r''+V_\theta''V_\theta'')\end{aligned} \tag{10}$$

$$V_\theta=W_\theta+\omega r \tag{11}$$

In above equations, ω is the rotation speed. And τ_{ij} is the Reynolds stress tensor as followings:

$$\tau_{ij}=\mu\left(2S_{ij}-\frac{2}{3}\delta_{ij}(\nabla\cdot\vec{V})\right) \tag{12}$$

$$\delta_{ij}=\begin{cases}1 & (i=j)\\ 0 & (i\neq j)\end{cases} \tag{13}$$

$$S_{ij}=\begin{bmatrix}\dfrac{\partial V_x}{\partial x} & \dfrac{1}{2}\left(\dfrac{\partial V_x}{\partial r}+\dfrac{\partial V_r}{\partial x}\right) & \dfrac{1}{2}\left(\dfrac{\partial V_x}{r\partial\theta}+\dfrac{\partial V_\theta}{\partial x}\right) \\ \dfrac{1}{2}\left(\dfrac{\partial V_x}{\partial r}+\dfrac{\partial V_r}{\partial x}\right) & \dfrac{\partial V_r}{\partial r} & \dfrac{1}{2}\left(\dfrac{\partial V_r}{r\partial\theta}+\dfrac{r\partial}{\partial r}\dfrac{V_\theta}{r}\right) \\ \dfrac{1}{2}\left(\dfrac{\partial V_x}{r\partial\theta}+\dfrac{\partial V_\theta}{\partial x}\right) & \dfrac{1}{2}\left(\dfrac{\partial V_r}{r\partial\theta}+\dfrac{r\partial}{\partial r}\dfrac{V_\theta}{r}\right) & \dfrac{\partial V_\theta}{r\partial\theta}+\dfrac{V_r}{r}\end{bmatrix} \tag{14}$$

$$\mu=\mu_l+\mu_t,\ \ \lambda=\frac{\mu_l c_p}{p_r}+\frac{\mu_t c_p}{p_{rt}} \tag{15}$$

The laminar flow viscosity μ_l is obtained from Sutherland's law and the turbulent flow viscosity μ_t is obtained from the mixing length turbulence model [19].

For unsteady simulation, the dual time stepping approach is used. The second order 3-point Euler backward scheme is used for physical time discretization and the explicit SCREE scheme is employed for pseudo temporal discretization. Local time stepping, implicit residual smoothing and multigrid are employed to accelerate the convergence. The second order central scheme with addition of second and fourth order artificial dissipation is used for space discretisation. The mixing plane method [17] is employed in the steady simulation and the continuous interface plane method [4] in the time-averaging simulation. The domain scaling method is employed in the unsteady simulation. More details about the solution method can be found in the reference [18].

1.2 Exponential Decay DC Model

In our previous studies [12,14], the distribution characteristics of DC and the effects of DC on time-averaging simulation were conducted in axial compressors.The main conclusions related to DC modelling are as followings: 1)The DC has large magnitudes at the rotor-stator interface and decreases rapidly in flow direction from the interface. 2) The time-averaging simulation with axisymmetric DC can take into account the major part of the unsteady effects on spanwise redistribution. 3) Either DS or DEF can only reproduce a partial influence of unsteady blade row interactions. Hence, both DS and DEF should be modeled in the APES approach.

Based on above results and other studies [20-22], an exponential decay DC model for downstream blade row is proposed as following.

$$f_i'' f_j''(s,r) = f_i'' f_j''(s,r)\Big|_{ref} \bullet fun1 \bullet fun2 \bullet \left(\frac{W_s}{W_{s_{ref}}}\right)^2 \tag{16}$$

$$\begin{cases} fun1 = e^{(-\frac{s-s_{ref}}{c_1 L})} & s<s_{le} \\ fun1 = e^{(-\frac{s_{le}-s_{ref}}{c_1 L})} & s \geq s_{le} \end{cases} \tag{17}$$

$$\begin{cases} fun2 = 1 & s<s_{le} \\ fun2 = e^{(-\frac{s-s_{le}}{c_2 L})} & s \geq s_{le} \end{cases} \tag{18}$$

$$s_{le} = L + c_3 L \tag{19}$$

Where $f_i'' f_j''(s,r)$ represents local DC and subscript ref represents the reference point. L is the meridional distance from upstream blade row trailing edge to downstream blade row leading edge. And s is the meridional distance downstream from the upstream blade row trailing edge. W_s and $W_{s_{ref}}$ is axisymmetric averaged velocity at local and reference points to account for pressure gradient. c_1, c_2 and c_3 are empirical coefficients and set to 0.5, 1.0 and 0.25 respectively based on the test case.

Usually reference point is set at interface plane or 1-3 grid points upstream from interface plane. Then $f_i'' f_j''(s,r)\Big|_{ref}$ could be calculated based on circumferential distribution of flow fields at (s,r) in the upstream blade row by using spatial-temporal transformation [8]. The whole DC in the downstream passage can be obtained according to the exponential decay model. Though the model is proposed for DC in downstream blade row to account for the unsteady effects of upstream blade row, it could give reasonable DC in upstream blade row. For upstream blade row, s is the meridional distance upstream from the downstream blade row leading edge and reference point is set at interface plane or 1-3 grid points downstream from interface plane.

Then the DC model was added into the developed time-averaging CFD flow solver. There is only a little increase (less than 1%) in CPU time owing to the addition of the DC model.

1.3 Test Case

In this paper, the first transonic compressor stage of NASA 67 was used to validate the proposed model [23]. The design rotation speed is 16042.8 rpm, and the total pressure ratio is 1.59. It consists of 22 rotor blades and 34 stator blades. More design details can be seen in the reference [23]. In this study, stator blade row was moved upstream close to the rotor blade, resulting that the axial gap between rotor and stator is 10 mm at hub, in order to highlight the UBRI.

Steady, unsteady and time-averaging simulations, employing the developed flow solver, were conducted. The unsteady simulation was simplified by modifying the original blade row airfoil counts from 22: 34 to 22: 33. Then the computational domain consists of 2 rotor blade passages and 3 stator blade passages. The dual time stepping approach was used for unsteady simulation. The number of physical time steps was set to 72 for each cycle and the maximum number of inner iterations was set to 150 for each physical time step. The steady and time-averaging simulations were conducted with one rotor passage and one stator passage, and were about 80 times faster than the unsteady simulation with two rotor passages and three stator passages. Two kinds of time-averaging simulations were carried out using exponential decay DC model and DC derived from the unsteady simulation, respectively.

The same grid distribution was given based on the experience employing the Denton's code using mixing length turbulence model. As shown in Figure 1, the grid is 37, 41 and 141 in pitchwise, spanwise and streamwise direction respectively for one rotor or stator passage. The grid density is similar to the reference [24] for investigating the DLR compressor stage by steady, unsteady and nonlinear harmonic methods.

Total pressure, total temperature and inlet flow angles were specified for the inlet boundary, whereas the static pressure was imposed according to the simple radial equilibrium equation for the outlet boundary. Adiabatic conditions were adopted for all the solid walls.

The flow was assumed to be fully turbulent in the computations.

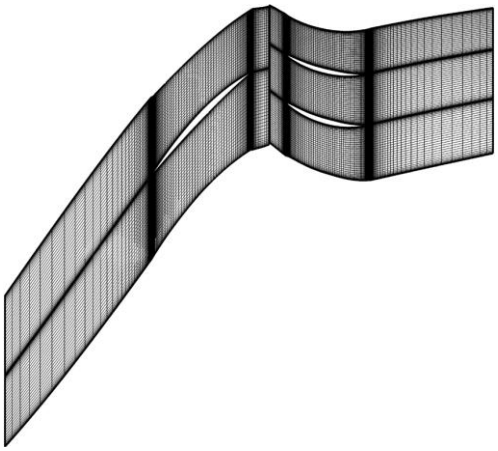

(a) S1 flow plane at 50% span

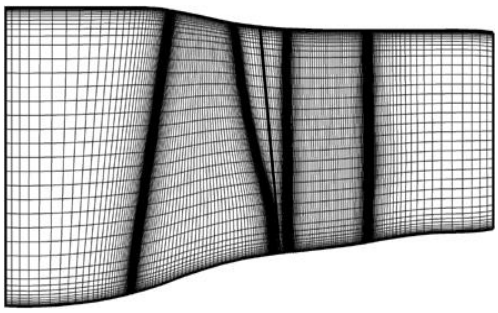

(b) Meridional plane

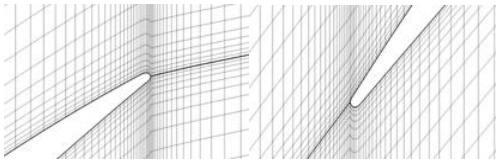

(c) Leading and trailing edge of rotor in (a)

Figure 1. Computational grid

2. RESULTS AND DISCUSSION

The results from steady and unsteady simulations are firstly compared. It is found that the steady simulation with mixing plane method can predict the total performance of the single axial compressor well in comparison with the unsteady result for design condition. However, the spanwise distribution of total pressure, total temperature, entropy and Mach number predicted by steady mixing plane method has some discrepancies with the unsteady results (shown later).

In the paper, DesIJ and QesHI represent DS and DEF. And I, J could be R, T or X (R, T and X stand for spanwise, pitchwise and streamwise). For example, DesRT and QesHT represents $\overline{\rho}V_r''V_\theta''$ and $\overline{\rho}H''V_\theta''$ respectively.

2.1 DC Analysis

As discussed above, the DC could present the effect of UBRI on time-averaged flow, and how to model the DC is the key in the APES method. The DC can be derived from unsteady simulations directly.

UBRI is a result of potential interaction, vortical interaction (associated with wakes, tip leakage vortex, passage vortices) and shockwave interaction. Figure 2 presents an instantaneous entropy contours at mid span from unsteady simulation. It indicates clearly the rotor wake chopping, stretching and migrating in the downstream stator passage. The circumferential and spanwise transport of wake leads to a circumferential and spanwise redistribution of total temperature and momentum. And accounting for spanwise redistribution is very important in predicting the aerodynamic performance of multistage axial flow compressors.

Figure 3 shows one dimensional distributions of area averaged DC for the whole s3 plane along flow direction in the rotor and stator passage respectively. It is found that DC in the stator is much larger than that in the rotor, which also indicates that the unsteady interaction has much larger effect on the stator than on the rotor for this transonic fan. Hence, later analysis is focused on stator. DC has large magnitudes at the rotor-stator interface and decreases rapidly in flow direction from the interface, especially in the rotor-stator gap. It presents exponential decay characteristic that will be shown later.

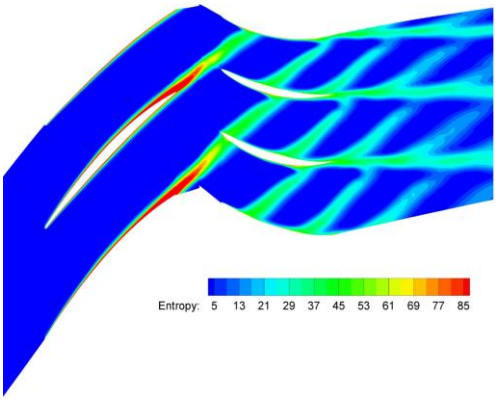

Figure 2. Instantaneous entropy contours at mid span

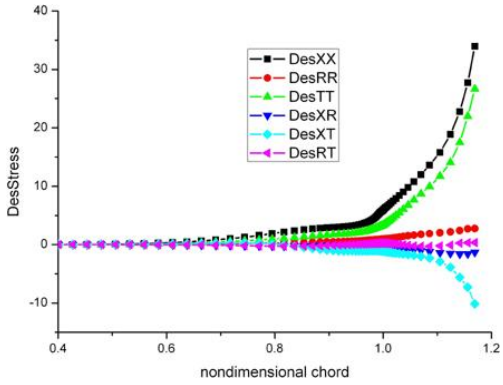

(a) DS in the rotor passage

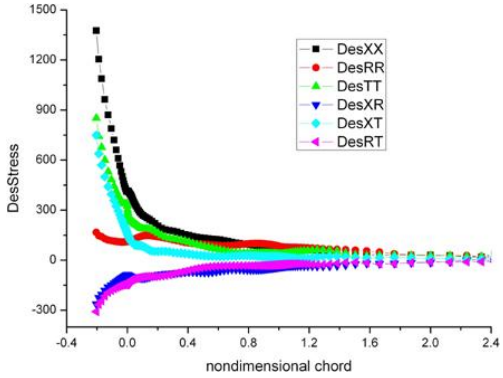

(b) DS in the stator passage

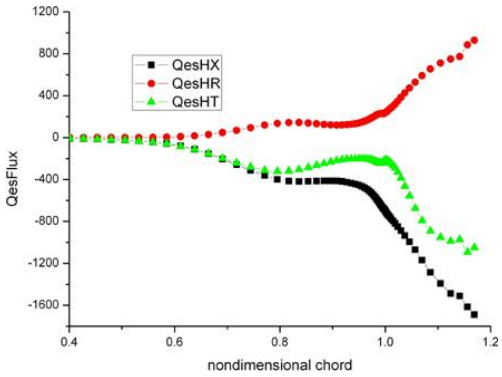

(c) DEF in the rotor passage

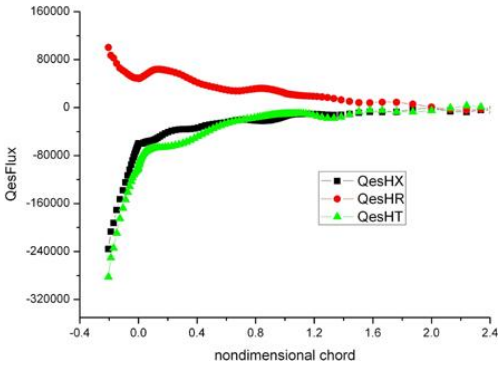

(d) DEF in the stator passage

Figure 3. DC distribution along flow direction

2.2 Validation of Exponential Decay DC Model

How to model the DC to close the equation system is the key in the APES. Hence, firstly the DC distributions resulted from the DC model are compared with the ones from unsteady simulation. Then mean flow fields from steady simulation, time-averaging simulations with the DC model and the DC derived from the unsteady simulation are compared.

2.1.1 DC Comparisons

In this section, the DC distributions resulted from the DC model are compared in detail with the ones from unsteady simulation. We should note that all these DC terms are set zero in steady simulation with mixing plane method.

Figure. 4 and Figure. 5 present circumferential averaged $\overline{\rho}V_x''V_x''$ and circumferential averaged $\overline{\rho}V_x''H''$. The results show that the DC in stator passage are much larger than the DC in rotor passage. The DC decay quickly from the rotor-stator interface plane in the downstream stator. Compared with unsteady results, the proposed exponential decay DC model could predict reasonable DC distribution qualitatively. Figure. 6 and Figure. 7 present circumferential averaged $\overline{\rho}V_x''V_x''$ and circumferential averaged $\overline{\rho}V_x''H''$ at 10%, 50% and 90% span along chord in the stator passage. The comparisons indicate that the DC model could predict reasonable DC distribution quantitatively.

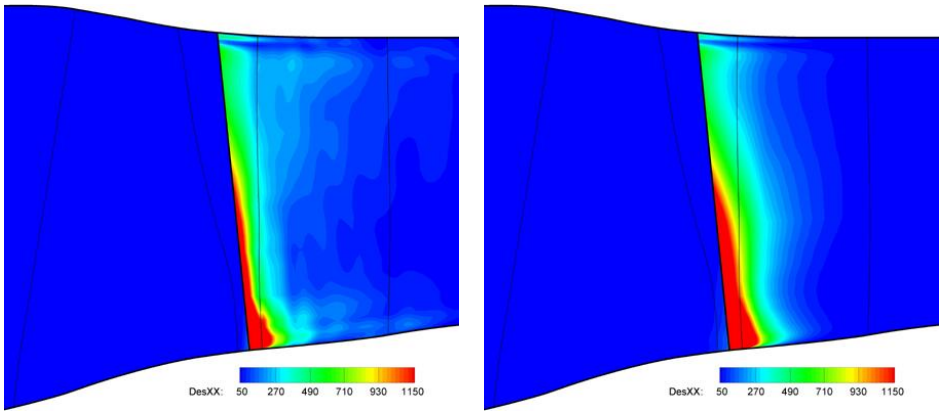

(a) Unsteady (b) Model

Figure 4. Circumferential averaged $\overline{\rho}V_x''V_x''$

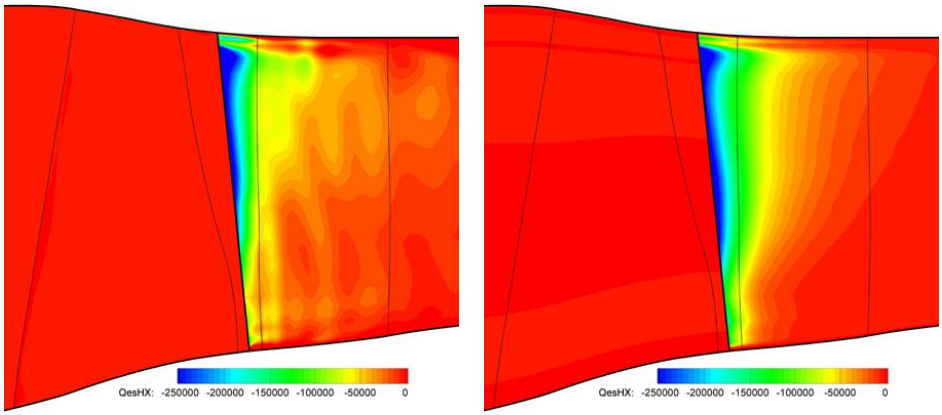

(a) Unsteady (b) Model

Figure 5. Circumferential averaged $\overline{\rho}V_x''H''$

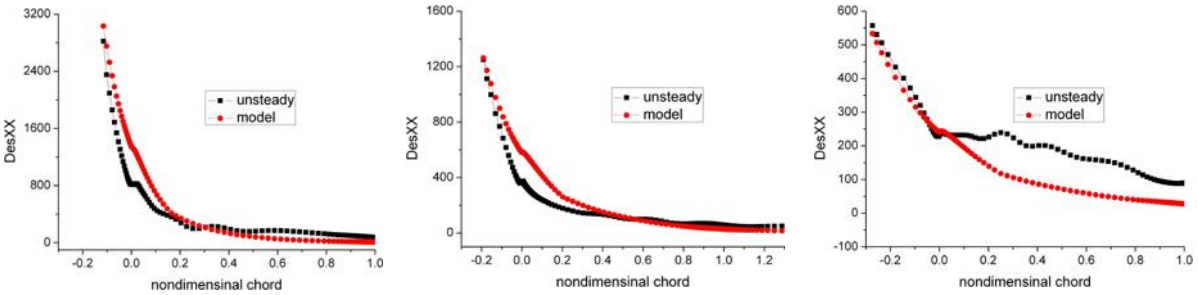

(a)10% span (b) 50% span (c) 90% span

Figure 6. Circumferential averaged $\bar{\rho}V_x''V_x''$ along chord in the stator passage

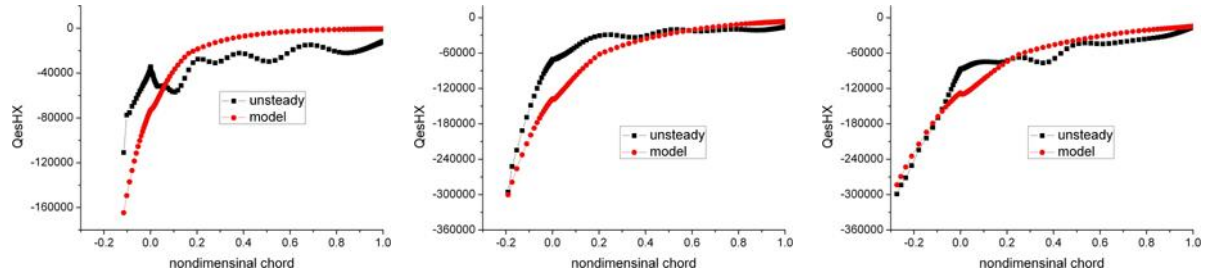

(a)10% span (b) 50% span (c) 90% span

Figure 7. Circumferential averaged $\bar{\rho}V_x''H''$ along chord in the stator passage

2.1.2 Mean Flow Fields

To further validate the proposed exponential decay DC model, the results from steady simulation (named st), time-averaging simulation with the DC model (named model) and time-averaging simulation with the DC derived from the unsteady simulation (named dqe) are compared.

Figure. 8 present spanwise distributions of circumferential averaged total pressure, total temperature and Ma at the stator exit. Though there are still some discrepancies near hub region, the exponential decay model could predict the spanwise distributions of flow parameters well. This indicates that the model can take into account the major part of UBRI and provide significant improvements for predicting spanwise distributions of flow properties in axial compressors, compared with the steady mixing plane method.

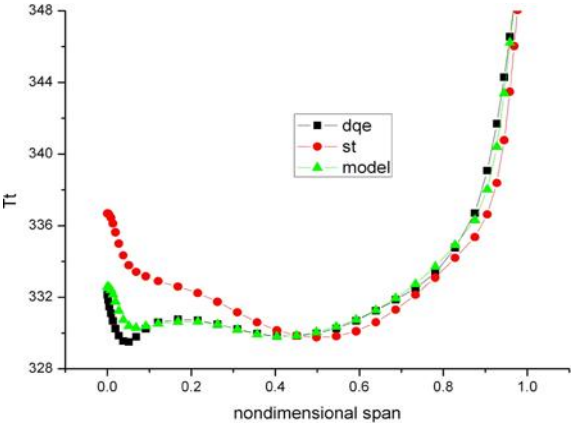

(b) Total temperature

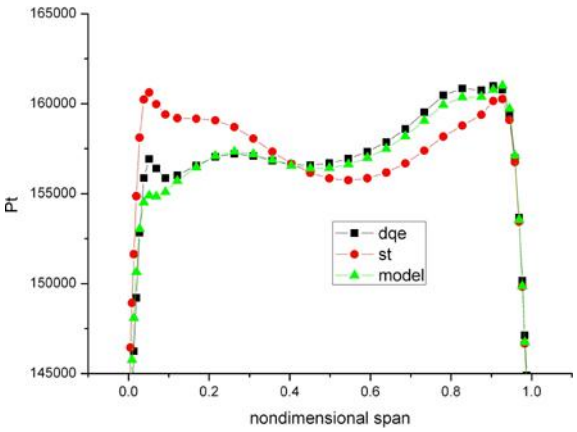

(a) Total pressure

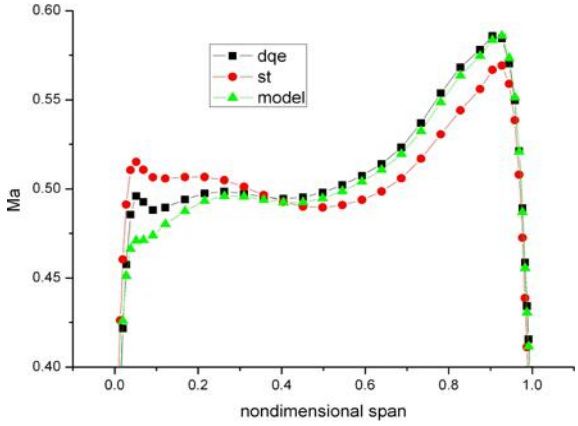

(c) Ma

Figure 8. Comparison of total pressure, total temperature and Ma at the stator exit

3. CONCLUSIONS

To develop a DC model for compressor routine design, a 3D viscous unsteady and time-averaging CFD flow solver is developed. Steady, unsteady and time-averaging simulations are conducted on the investigation of the UBRI in the first stage of NASA 67 compressor.

Based on DC characteristics and its effects on time-averaged flow, an exponential decay DC model is proposed and implemented into the time-averaging solver. There is only a little increase (less than 1%) in CPU time owing to the addition of the DC model.

Based on the unsteady simulation, the proposed model is validated by comparing DC distributions and mean flow fields. The comparisons indicate that the DC model could predict reasonable circumferential averaged DC distribution quantitatively. Furthermore, the model can take into account the major part of UBRI and provide significant improvements for predicting spanwise distributions of flow properties in axial compressors.

ACKNOWLEDGMENTS

This work is supported by the National Natural Science Foundation of China (No. 51376001, No. 51676007, No. 51420105008), the National Basic Research Program of China (No. 2014CB046405). Yangwei Liu is supported by the China Scholarship Council (CSC) for a one-year visit to the University of Cambridge.

REFERENCES

[1] J. D. Denton. Some Limitations of Turbomachinery CFD. ASME paper GT2010-22540, 2010.

[2] J. J. Adamczyk. Model equations for simulating flows in multistage turbomachinery. ASME paper 85-GT-26, 1985.

[3] J. J Adamczyk, R. A. Mulac, M. L. Celestina. A Model for closing the invisid form of the average passage equation system. Journal of Turbomachinery. 108, 180-186,1986.

[4] C. M. Rhie, A. J. Gleixner, D. A. Spear. C. J. Fischberg, R. M. Zacharias. Development and application of a multistage Navier-Stokes solver-Part I: Multistage modeling using bodyforces and deterministic stresses. Journal of Turbomachinery. 120, 205-214, 1998.

[5] Y. G. Li and A. Tourlidakis. Influence of deterministic stresses on flow prediction of a low-speed axial flow compressor rear stage. IMechA. 215, 571-583, 2001.

[6] D. L. Sondak, D. J. Dorney, R. L. Davis. Modeling turbomachinery unsteadiness with lumped deterministic stresses. AIAA paper 96-2570, 1996.

[7] L. He. Modeling issues for computation of unsteady turbomachinery flows. Unsteady Flows in Turbomachines, von Karman Inst. Lecture Series 1996-05, von Karman Inst. for Fluid Dynamics, Rhode Saint Genese, Belgium, 1996.

[8] E. J.Hall: Aerodynamic modeling of multistage compressor flow fields. Part II: modeling deterministic stresses. ASME paper 97-GT-345, 1997.

[9] A. G. van de Wall. A transport model for the deterministic stresses associated with turbomachinery blade row interactions. Ph.D. Thesis, Department of Mechanical and Aerospace Engineering, Case Western Reserve University,1999.

[10] D. Charbonnier and F. Leboeuf: Steady flow simulation of rotor-stator interactions with a new unsteady flow model. AIAA paper 2004-3754, 2004.

[11] S. Stollenwerkl, E. Kugeler. Deterministic stress modeling for multistage compressor flowfields. ASME paper GT2013-94860, 2013.

[12] Y W Liu, B J Liu, L P Lu. Study of modeling unsteady blade row in-teraction in a transonic compressor stage part 1: code development and deterministic correlation analysis. Acta Mech Sin, 28: 281–290, 2012.

[13] Y W Liu, B J Liu, L P Lu. Investigation of unsteady impeller-diffuser interaction in a transonic centrifugal compressor stage. ASME paper GT2010-22737, 2010.

[14] Y W Liu, B J Liu, L P Lu.. Study of modeling unsteady blade row in-teraction in a transonic compressor stage part 2: influence of deter-ministic correlations on time-averaged flow prediction. Acta Mech Sin, 28: 291–299, 2012.

[15] B J Liu, B Zhang, Y W Liu. Numerical investigations of impeller–diffuser interactions in a transonic centrifugal compressor stage using nonlinear harmonic method. Proceedings of the Institution of Mechanical Engineers, Part A: Journal of Power and Energy, 228(8): 862-877, 2014.

[16] B J Liu, B Zhang, Y W Liu. Investigation of model development for deterministic correlations associated with impeller-diffuser interactions in centrifugal compressors[J]. Science China Technological Sciences, 2015, 58(3): 499-509.

[17] J. D. Denton. The calculation of 3d viscous flow through multistage turbomachines. Journal of Turbomachinery. 114, 18-26, 1992.

[18] Y. W. Liu. Investigations of steady state numerical techniques for predicting flows through multistage compressors. Ph.D Thesis, Beijing University of Aeronautics and Astronautics, 2009.

[19] J. D. Denton. The use of body force to simulate viscous effects in 3D flow calculations. ASME Paper 86-GT-144, 1986.

[20] Hathaway M. D., Suder K. L., Okiishi T. H., et al. Measurements of the Unsteady Flow Field within the Stator Row of a Transonic Axial-Flow Fan-Results and Discussion. NASA Technical Report 86-C-31, 1987

[21] O. Uzol, Y.-C. Chow, J. Katz, et al. Average Passage Flow Field and Deterministic Stresses in the Tip and. Hub Regions of a Multi-Stage Turbomachine. ASME Journal of Turbomachinery, 125(4): 714-725, 2003

[22] C. Poensgen, H. E.Gallus. Three-dimensional Wake Decay inside of a Compressor Cascade and its Influence on the Downstream Unsteady Flow Field-Part 1: Wake Decay Characteristics in the Flow

Passage. ASME paper 90-GT-21, 1990.

[23] D. C. Urasek, W. T. Gorrell, W. S. Cunnan. Performance of two-stage fan having low-aspect-ratio first-stage rotor blading. NASA TP-1493, 1979.

[24] T. Chen, P. Vasanthakumar and L. He. Analysis of unsteady blade row interaction using nonlinear harmonic approach. Journal of Propulsion and Power, 17(3), 651-658, 2001.